

Advances in Natural Science  
Vol. 3, No. 2, 2010, pp. 225-234  
[www.cscanada.net](http://www.cscanada.net)

ISSN 1715-7862 [PRINT]  
ISSN 1715-7870 [ONLINE]  
[www.cscanada.org](http://www.cscanada.org)

 \*The 3rd International Conference of Bionic Engineering\*

## Micro-tensile Testing of the Lightweight Laminated Structures of Beetle Elytra Cuticle<sup>1</sup>

SUN Ji-yu<sup>2</sup>

TONG Jin<sup>3</sup>

CHEN Dong-hui<sup>4</sup>

LIN Jian-bin<sup>5</sup>

LIU Xian-ping<sup>6</sup>

WANG Yue-ming<sup>7</sup>

**Abstract:** Quantitative measurements of the mechanical properties of insect cuticle are a useful tool in the development of bio-mimetic materials suitable for industrial products. In this study, a micro-tensile tester was used to investigate the mechanical properties of elytra cuticle of the dung beetle (*Copris ochus* Motschulsky). Micro tensile testing show that: yield strength ( $F_s$ ) = 17.12±3.55N, Maximum tensile ( $F_b$ ) = 14.74±4.11N, yield strength ( $\sigma_s$ ) = 1.4±0.15GPa, tensile strength ( $\sigma_b$ ) = 1.2±0.21GPa, elastic modulus ( $E$ ) = 14.56±4.20GPa, plastic index ( $\delta$ ) = 0.241±0.10. Tensile elongation of the specimens was between 12.1-36.3%. Our results demonstrate that the elytra possess ductile material characteristics. Field emission scanning electron microscopy (FESEM) was used to investigate the detailed structure of the elytra cross section in both the transverse and longitudinal directions. In the transverse direction, the fibers of the deeper layers of the endocuticle are orientated in a constant, rotated angle with neighboring fibers rotated in relation to the each other in the same direction. The fibers in the longitudinal direction show that the epicuticle, exocuticle and endocuticle layers clearly create a parallel hierarchical structure. We believe this is a result of the composite effect of the hierarchical structure. Finally, we developed a laminated model based on the parameters

<sup>1</sup> This work was supported by National Natural Science Foundation of China (grant no.30600131), by the Science & Technology Development Projects of Jilin Province (grant no.20090147, 20090711), by the Basic Operation Foundation of Jilin University (grant no.200903271), the National Hi-tech Project (863 Project) (grant no.2009AA043604-2) and by "Project 985" of Jilin University.

<sup>2</sup> Corresponding author, Key Laboratory of Bionic Engineering, Ministry of Education, China, Jilin University, PR China.

<sup>3</sup> Key Laboratory of Bionic Engineering, Ministry of Education, China, Jilin University, PR China.

<sup>4</sup> Key Laboratory of Bionic Engineering, Ministry of Education, China, Jilin University, PR China.

<sup>5</sup> Key Laboratory of Bionic Engineering, Ministry of Education, China, Jilin University, PR China.

<sup>6</sup> School of Engineering, the University of Warwick, UK.

<sup>7</sup> Key Laboratory of Bionic Engineering, Ministry of Education, China, Jilin University, PR China.

\*Received 7 May 2010; accepted 19 July 2010

provided by tensile testing, FESEM imaging and nanoindentation measurements, and compared the results of the model to our experimental results.

**Key words:** nanoindentation; micro-tensile testing; coupled analysis; laminated structure

## 1. INTRODUCTION

Many biological systems have mechanical properties that are far beyond those that can be achieved using synthetic materials manufactured with present technology. This superiority is possible because biological organisms can produce composites that are organized in terms of composition and structure, containing both inorganic and organic components in complex structures hierarchically organized at the nano-, micro-, and meso-levels (Meyers et al., 2006). Natural biomaterials can have unique structures and functions because of their evolution through the exchange of energy, matter and information with their surroundings over millions of years. Based on the structures of natural biomaterials, biomimetic materials have been developed (George & Mehmet, 2004).

The cuticle represents 25% of the dry weight of the entire insect body. It is resilient, waterproof and lightweight; an excellent crude composite material. It not only supports the insect, but also gives the insect its shape, means of locomotion, waterproofing and a range of mechanical tricks (Vincent, 2002). It is preternaturally multifunctional since the cuticle has to perform all the functions of skin and skeleton (Vincent, 1999).

Insect cuticle structures have been analyzed previously (Scherge & Gorb, 2002; Wegst & Ashby, 2004), and this research has shown that the cuticle surface of dung beetles has a laminated composite structure. The cuticle consists of three main layers: the epicuticle, the exocuticle and the endocuticle, where the latter two layers form the procuticle. Since nearly all adult insects can fly, the cuticle has to provide a very efficient and lightweight skeleton (Vincent & Wegst, 2004). A widely accepted theory is that insect cuticle is a composite consisting of chitin fibers and a proteinaceous matrix in a layered structure (Vincent, 2002; Wegst & Ashby, 2004).

The mechanical properties of insect cuticle may provide clues to the design of advanced composites. However, due to the micro or nanoscale of insect cuticle thickness, only tensile tests could be conducted until nanoindentation techniques were developed. The nanoindenter provides an approach for assessing the mechanical properties in microelectronic devices and films based on quantitative, controlled nanoindentation of surfaces, with the convenience of modern automation. It is also suitable to measure the mechanical properties of biomaterials (Sarikaya et al., 2002; Haque, 2003).

Studies of nanoindentation properties in a variety of insects have been recently conducted. To understand the effect of desiccation and the outer wax layer on the mechanical behavior of biomaterial, the gula plate of the beetle *Pachnoda marginata* was tested in fresh, dry and chemically treated conditions using a nanoindenter. It was found that desiccation has a strong influence on the nanoindentation results (Barbakadze et al., 2006). The exoskeleton of the ground beetle *Scarites subterraneus* was tested using nanoindentation where it was found that the hardness and reduced elastic modulus at the mandible were much higher than those at the abdomen (Michelle). This result may be due to an increased level of heavy metals and halogens, such as zinc (Zn) and manganese (Mn), incorporated into the nanoscale structure of the exoskeleton during maturation, and likely correlates to the different functions of fighting and protection of the two areas. A quasistatic nanoindentation technique was used to measure cuticle stiffness of live *Drosophila melanogaster* during its larval, pupal, and early adult development *in vivo* (Michelle) and the cuticle was found to exhibit viscoelastic behavior.

This paper analyzes the morphology, microstructure, and tensile characteristics of the beetle elytra cuticle. This analysis will be combined with a determination of the cuticle's nanomechanical properties coupled with a finite element method to establish a laminated sandwich structure model and a finite element

analysis. The results of this study will inspire new ideas in developing high-performance composite material designed to provide superior electromechanical properties.

## 2. MATERIALS AND METHODS

### 2.1 Specimens

Living dung beetles (*Copris ochus*) were collected in the suburb of Changchun, Jilin Province, China. Fig. 1a shows a photograph of a female dung beetle with the arrow pointing to the elytra. Elytra are a pair of hard forewings which protect the hind wings and the body of the beetle. The bodies of the collected beetles were 20-30 mm in length and approximately 16 mm in width. The Wyko NT9100 Optical Profiler was used to measure the surface morphology of the elytra, which showed longitudinal node grooves in the surface and accumulations of some substance in the nodes. The depth of the grooves is in the range of 6.62~14.04  $\mu\text{m}$  which has a beneficial aerodynamic effect (shown in Fig. 1b and 1c). The groove depths gradually become shallower, and are higher in middle part than at the edge. This groove configuration provides high aerodynamic stability combined with low mass.

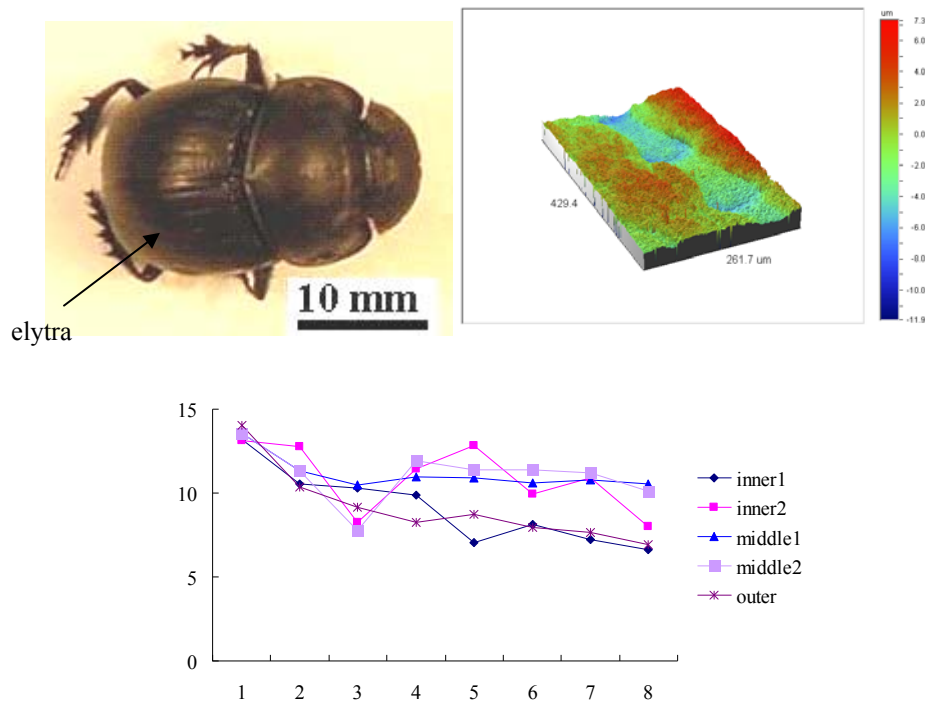


**Fig.1: a) Photograph of one female dung beetle *Copris ochus* Motschulsky (the arrow shows the elytra part); b) the 3D image of groove of elytra; c) the depth of groove from head to tail.**

The living beetles were dissected on a cotton surface to prevent contamination. The elytra were first severed from the beetle and then prepared for analysis. With a tensile test, it is important to provide the external force through the specimen axis to ensure that the material is in a tensile state; therefore, the specimen geometry must be in accordance with an aspect ratio of length with width greater than 5 or 10 preparation. Due to size and shape restrictions of the elytra, only a longitudinal specimen preparation of the elytra provided the necessary geometry for the application of external force. From each beetle, a 15 x 3 mm specimen was obtained by first cutting vertically with scissors in the Y direction, then cutting two V-shapes in the middle along the horizontal x-axis to ensure that the fracture occurred away from the chuck. The schematic diagram of the procedure and the specimen graph are shown in Fig. 2.

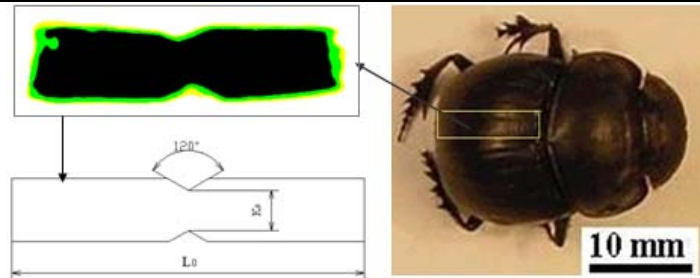


Fig. 2: The schematic diagram and specimen graph of elytra of dung beetle

The fracture analysis diagram for each specimen was acquired using a Field Emission Scanning Electron Microscope (FESEM, XL30 ESEM-FEG). The fracture section was treated with a gold spray and placed within the FESEM for analysis and photographs.

## 2.2 Micro-tensile tester

The micro-tensile test used a MTEST 300 tensile test unit that is a corollary analysis tool for the FESEM (shown in Fig. 3). The apparatus is equipped with a telescopic instrument that can accurately provide resistance at all stages of linear elongation, and the optical encoder can accurately measure the tensile (compression) speed. The principle experimental specimens were placed in the ends of a horizontal clamping jaw (fixture), with the stainless steel sliding providing support. A box in the lower part contains two motor driven pulleys which provided the external force; a double-threaded, screw-driven fixture at both ends move in the opposite directions with a dimensional precision of 0.001 mm. After the tensile test, a FESEM observation of the fracture surface characteristics of specimens was performed to determine the stress concentration and the notch effect on the impact fracture.

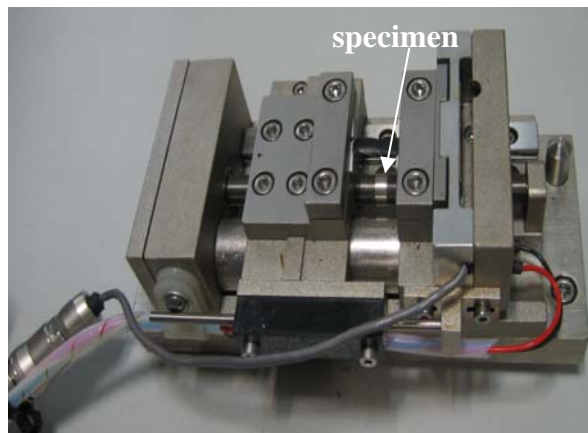


Fig. 3: Tensile Test Units (MTEST 300 module)

## 3. RESULTS AND DISCUSSION

### 3.1 Tensile test

To determine the validity of the FEM model, micro-tensile tests were performed on the elytra cuticle. The relationship of strain and stress of the elytra is shown in Fig. 4. The tensile curve goes through a steady increase in the first stage, then rapidly declines before remaining stable (with a slight increase) after the plastic deformation fracture. The elytra's macro-deformation characteristics are somewhat similar to the tensile curve of ductile materials. There is a local maxima point of instability due to the geometric effect; that is, there are bottlenecks as a result of the specimen and the various deformations concentrated in the region.

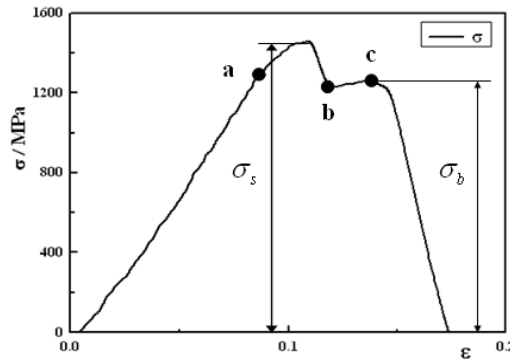


Fig. 4: The relationship of strain and stress of elytra

The testing was carried out on a total of 12 groups of elytra; because of differing specimen sizes and other operational factors there are some differences in the tensile process and results between specimen groups, as shown in Table 1.

Table 1: Tensile difference on effect and cause analysis

group	fracture position	maximum strain	reason
1(8)	Intermediate notch	0.363	Test results normal.
2(3)	The tail of elytra, near the gripping department approximately 3mm	0.485	Elytra tail is hard and brittle with greater curvature, the thickness of relatively thin, so may occur a crack or injury when preparation of specimen.
3(1)	Tail clamping Department	0.180	Specimen was crushing because the elytra tail too thin.

The numbers in parentheses are the number of emerging.

The specimens with the fracture occurring in the intermediate notch were designated as the effective data and consisted of 8 specimens. The thickness of the specimen before and after the test was unchanged. The image analysis system (OLYCIA™M3) was used to measure the vertical thickness of the tensile section and take the mean value of thickness. Pre-test specimen sizes are shown in Table 2.

Table 2: The specimen size before the tensile test

specimens	$L_0$ /mm	$K_0$ /mm	$A_0$ / $mm^2$
1	15.2	2.4	0.012
2	15.0	2.7	0.014
3	15.1	2.2	0.011
4	14.2	2.0	0.010
5	15.8	2.6	0.013
6	15.3	2.8	0.014
7	15.2	2.4	0.012
8	15.6	2.2	0.011

$L_0$ , Original gauge length;  $K_0$ , between the notch width;  $A_0$ , Notch part sectional area.

The plastic index of materials is usually expressed as the residual deformation after specimen fracture, where the plastic index used in static uniaxial tension is expressed as the elongation after fracture  $\delta$  and reduction of area  $\psi$ . Because the thickness of the specimen is at the micron scale, which is very difficult to measure accurately, we only investigated  $\delta$ , defined as:

$$\delta = \frac{L_0 - L}{L_0} \times 100\% \quad (1)$$

Where  $L_0$  and  $L$  are the pre-tensile and post-fracture lengths, respectively.

The experimental results and  $\delta$  value are given in Table 3. The value of  $\delta$  is between 12.1-36.3% and the various stages of the tensile curves of the specimens are similar to that of materials of similar toughness. The accepted view is that an elongation of greater than 5% of the material after fracture is considered a ductile fracture; otherwise it is considered a brittle fracture. Given the evidenced fractures in our results, the elytra cuticle of the dung beetle can be considered a ductile material.

**Table 3: Tensile mechanical properties of the elytra cuticle**

specimens	$F_S$ /(N)	$F_b$ /(N)	$\sigma_S$ /(MPa)	$\sigma_b$ /(MPa)	$E$ /(GPa)	$\delta$
1	17.11	12.3	1425.83	1025.0	22.68	0.121
2	20.46	17.63	1461.43	1259.29	14.06	0.164
3	14.20	10.46	1290.91	950.91	10.02	0.188
4	13.33	11.17	1333.0	1117.0	16.85	0.342
5	20.26	19.20	1558.46	1476.92	14.75	0.152
6	21.40	20.50	1528.57	1464.28	10.20	0.241
7	18.08	16.14	1506.67	1345.0	11.54	0.360
8	12.09	10.52	1099.10	956.36	16.38	0.363
mean	17.12	14.74	1400.50	1199.35	14.56	0.241
standard deviation	$\pm 3.55$	$\pm 4.11$	$\pm 153.24$	$\pm 217.12$	$\pm 4.20$	$\pm 0.10$

### 3.2 Fracture morphology

The fracture morphology of the specimens after tensile deformation was directly observed using the stereomicroscope and FESEM. The fracture morphology of elytra is similar to a ductile fracture; sides have a relatively rough shear lip, interstitial cracks are caused by micro-serrated sections and the fractured part has a long fiber pull-out (shown in Fig. 5). All of these fracture phenomena point to high specimen toughness.

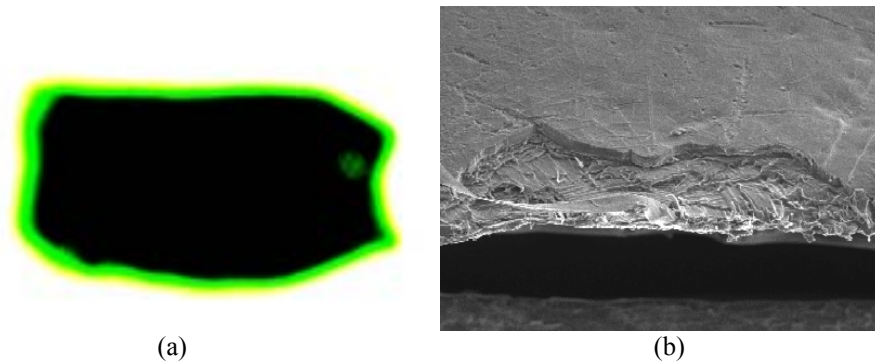


**Fig. 5: Specimen fractograph by the stereomicroscope (a) and FESEM (b)**

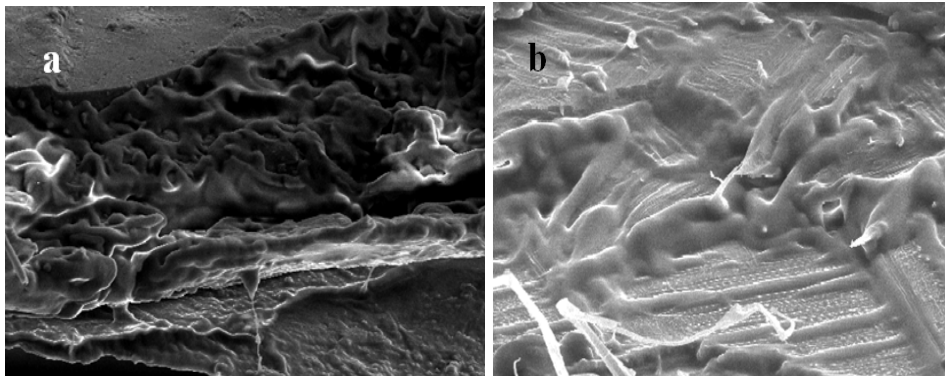


**Fig.6: Parabola-shaped dimples (a) and viscous flow-like plastic deformation (b)**

Fig. 6 illustrates two different kinds of fracture modes. A large number of hole-shaped dimples in the tensile fracture of the specimen had their edges clearly show tensile deformation. The larger contraction deformation exhibits a relatively high elongation (shown in Fig. 6a). Fig. 6b shows that the fracture has an obvious hierarchical structure and fiber breakage since a viscous, flow-like, polymer matrix plastic deformation occurred.

It can be seen that the fracture in the upper left corner has two obvious cracks. The fracture part has a large fiber-chip and tear where the matrix of the elytra epicuticle broke along the crack direction but did not completely separate. A large number of fiber-chip pull-outs and fractures show that the fiber disengaged from the matrix (shown in Fig. 7). This result is due to the mechanism of energy absorption, where the fiber is first separated from the crack, then from the matrix itself.

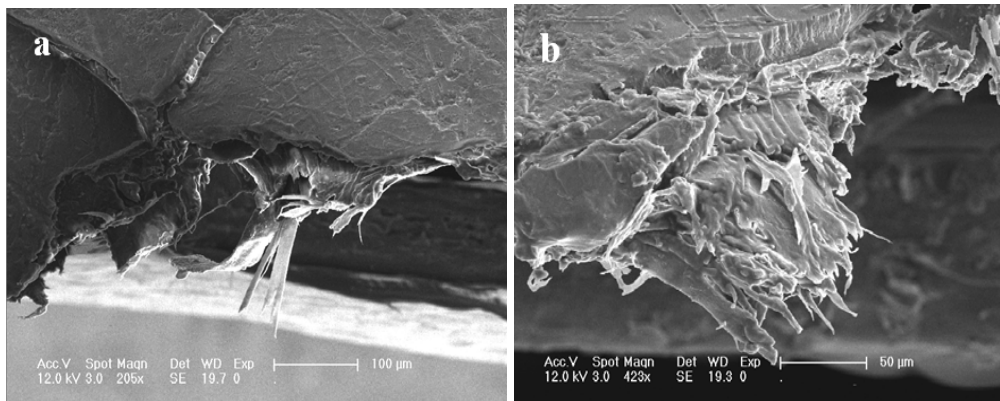


**Fig. 7: The fractograph in cracks part (a) and collapse photos (b) during tensile test**

Figure 8 shows the fracture mode occurring in different parts of elytra. The gap between the specimen fracture part and the structured layers of fracture and interlaminar interface have significant differences. In the fracture of the tail specimen, the composite layer structure is almost unobservable. Instead, there is a distribution of many fracture dimples and traces of irregular, slender fiber pull-outs. One possible reason for the fracture differences is that insect life requires different micro-structure within the parts of its body to provide differing functional needs.

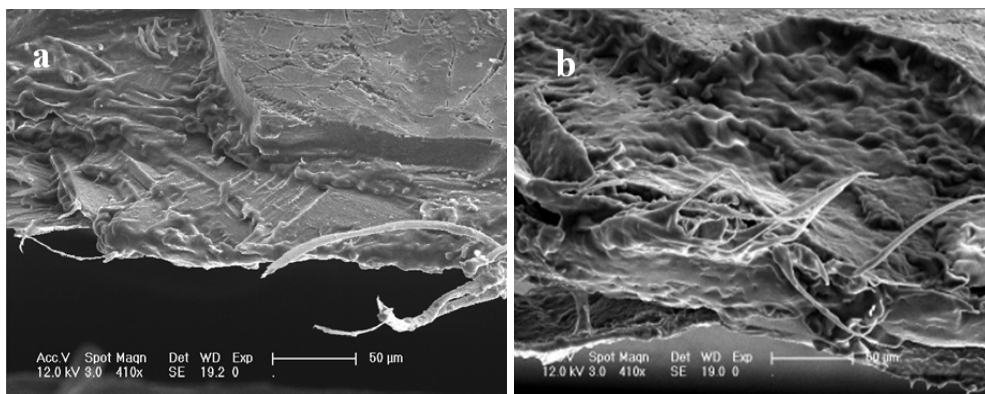


**Fig. 8: The fracture photograph of middle part (a) and tail part (b) of elytra**

Figures 9a and 9b show elytra without treatment after the tensile test by being directly placed into the FESEM to obtain *in vivo* fracture diagrams. Fig. 9c and 9d show specimens held at room temperature for one month (to allow for water loss) before the tensile test and observation in the FESEM. From the fracture results evident in Fig. 9a and 9b it can be seen that the composite layer sections are unformed. The matrix has a clear plastic deformation, fiber pull-out, and there are necking fracture traces. Figures 9c and 9d show that the composite layer is clearly stratified, with a cross-section formation perpendicular to the tensile

direction. The fiber fracture surface is smooth and there is separation between the matrices, showing that brittle fracture occurred in the specimen. This result shows that water losses can significantly affect the fracture properties of elytra enough that the material, which normally exhibits ductile fracture properties, can change to instead fracture in a brittle manner.

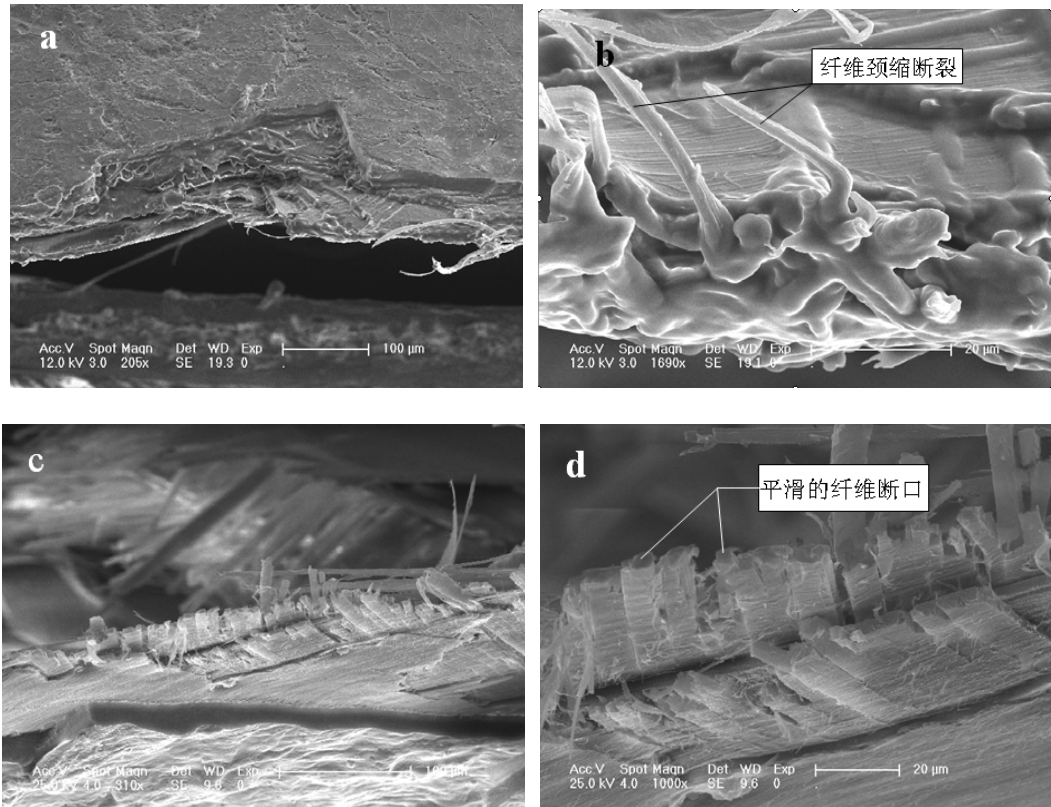


Fig.9: Two different fracture diagram *in vivo* (a,b) and water loss (c,d) condition

Structural biological materials are complex composites that have structures that are being extensively investigated by materials scientists and engineers with the ultimate goal of mimicking them in synthetic systems. This is indeed a new frontier in materials science and is a fertile ground for innovative and far-reaching work (Meyers et al., 2006). By visual analysis and mechanical properties tested by nanoindentation, our qualitative model was verified and will be helpful to the future analysis of the elytra cuticle and its reinforced hybrid-fiber composite structure.

## CONCLUSION

Natural biomaterials are multifunctional complex composites that possess a hierarchical structure. An increasing interest in the bionic design of materials based on structures of natural biomaterials has led to the nanomechanical characterization of biomaterials. This paper illustrates the structural composite of the elytra cuticle of the dung beetle *Copris ochus*. The cuticle's mechanical properties, reduced modulus and nanoscale hardness were investigated by using a micro-tensile tester and a nanoindenter. The tensile curve of the elytra cuticle is similar to that of other ductile materials, which can be divided into four stages: the elastic deformation step, the yield step, the strengthen step and the necking step. Reproducible fracture data from the middle of each specimen was obtained, with the following tensile properties:  $F_s=17.12\pm3.55\text{N}$ ,  $F_b=14.74\pm4.11\text{N}$ ,  $\sigma_s=1.4\pm0.15\text{GPa}$ ,  $\sigma_b=1.2\pm0.21\text{GPa}$ ,  $E=14.56\pm4.20\text{GPa}$ ,  $\delta=0.241\pm0.10$ . Tensile



elongation of the specimens was between 12.1-36.3%, verifying that the elytra cuticle can be considered a ductile material.

The fracture morphology of elytra cuticle is similar to that of a ductile fracture, in which parabola-shaped dimples and the viscous flow-like matrix of plastic deformation were found and indicate the toughness of the elytra material. In addition, it was found that the epicuticle of elytra dragged along the crack direction on the fracture part, causing the fiber to separate from the substrate and many fiber films to be pulled out and broken. We also found that water loss can significantly affect the fracture properties of elytra cuticle, making the cuticle fracture in a brittle manner rather than in the ductile manner previously seen. In addition, because of the gap effect and stress concentration effect, the agency's materials elongation and cross-section shrinkage rate was higher than that of the smooth parallel section, and a close inspection of the smooth uniform plastic deformation of the tensile elongation stage shows the potential for good gap plastic materials.

Details on the texture and inner construction of the elytra will be beneficial as it may motivate nano-texture research in new materials. Our future investigations will concentrate on extending the qualitative model we have established in order to find possible relationships between the structure and the mechanical properties of elytra cuticle which will be helpful for developing electromechanical composite materials for micro-aircraft, bionic tribology, bionic medical apparatus and bionic organs (tissue engineering).

## ACKNOWLEDGMENT

Thank for Mr. D. J. Robinson help us to investigate the surface morphology.

## REFERENCES

- Barbakadze N, Enders S, Gorb S, Arzt E. (2006). Local mechanical properties of the head articulation cuticle in the beetle *Pachnoda marginata* (Coleoptera, Scarabaeidae). *The Journal of Experimental Biology*, 209, 722-730.
- Bertram J E A, Gosline J M. (1987). Functional design of horse hoof keratin: the modulation of mechanical properties through hydration effects. *The Journal of Experimental Biology*, 130, 121-136.
- CHEN B, PENG X, WANG W, ZHANG J, ZHANG R. (2002). Research on the microstructure of insect cuticle and the strength of a biomimetic preformed hole composite. *Micron*, 33, 571-574.
- CHEN B, WU X Y. (2006). Analysis of Abnormal Fiber Shape of Chafer Cuticle. *Journal of Materials Science and Engineering*, 24, 683-686.
- CHEN P Y, LIN A Y M, LIN Y S, Seki Y, Stokes A G, Peyras J, Olevsky E A, Meyers M A, McKittrick J. (2008). Structure and mechanical properties of selected biological materials. *Journal of the Mechanical Behavior of Biomedical Materials*, 1, 208-226.
- George M, Mehmet S. (2004). Rigid biological composite materials: structural examples for biomimetic design. *Experimental Mechanics*, 42, 395-403.
- Haque F. (2003). Application of nanoindentation to development of biomedical materials. *Surface Engineering*, 19, 255-268.
- Hayes S A, Goruppa A A, Jones F R. (2004). Dynamic nanoindentation as a tool for the examination of polymeric materials. *Journal of Materials Research*, 19, 3298-3306.

- Kohane M, Daugela A, Kutomi H, Charlson L, Wyrobek A, Wyrobek J. (2003). Nanoscale *in vivo* evaluation of the stiffness of *Drosophila melanogaster* integument during development. *Journal of Biomedical Materials Research, A* 66, 633-642.
- Meyers M A, LIN A Y M, Seki Y, CHEN P Y, Kad B K, Bodde S. (2006). Structural biological composites: an overview. *JOM*, 58, 35-41.
- Meyers M A, CHEN P Y, LIN A Y M, Seki Y. (2008). Biological materials: structure and mechanical properties. *Progress in Materials Science*, 53, 1-206.
- Michelle, D. *Mechanical Properties of an Arthropod Exoskeleton*. [http://www.hysitron.com/page\\_attachments/0000/0413/Mechanical\\_Properties\\_of\\_an\\_Arthropod\\_Exoskeleton.pdf](http://www.hysitron.com/page_attachments/0000/0413/Mechanical_Properties_of_an_Arthropod_Exoskeleton.pdf)
- Olive W C, Pharr G M. (2004). Measurement of hardness and elastic modulus by instrumented indentation: advances in understanding and refinements to methodology. *Journal of Materials Research*, 19, 3-20.
- Saliba J E. (1996). Use of finite element in micromechanics of natural composites. *Computers & Structures*, 61, 415-420.
- Sarikaya M, FONG H, Sopp J M, Katti K S, Mayer G. (2002). Biomimetics: nanomechanical design of materials through biology. *15th ASCE Engineering Mechanics Conference*, New York, USA, pp.1-9.
- Scherge M, Gorb S N. (2002). *Biological micro- and nanotribology: nature's solutions*. Springer-Verlag Press, Berlin, 122.
- Skordos A, CHAN P H, Vincent J F V, Jeronimidis G. (2002). A novel strain sensor based on the campaniform sensillum of insects. *Philosophical transactions - Royal Society*, 360, 239-253.
- SUN J Y, TONG J, ZHOU J. (2006). Application of nano-indenter for investigation of the properties of the elytra cuticle of the dung beetle (*Copris ochus* Motschulsky). *IET Proceedings: Nanobiotechnology*, 153, 129-133.
- TONG J, SUN J Y, CHEN D H, ZHANG S J. (2004). Factors impacting nanoindentation testing results of the cuticle of dung beetle *Copris ochus* Motschulsky. *Journal of Bionic Engineering*, 1, 221-230.
- Vincent J F V. (2002). Arthropod cuticle: a natural composite shell system. *Composites Part A: Applied Science and Manufacturing*, 33, 1311-1315.
- Vincent J F V. (1999). From cellulose to cell. *The Journal of Experimental Biology*, 202, 3263-3268.
- Vincent J F V, Wegst U G K. (2004). Design and mechanical properties of insect cuticle. *Arthropod Structure & Development*, 33, 187-199.
- Wegst U G K, Ashby M F. (2004). The mechanical efficiency of natural materials. *Philosophical Magazine*, 84, 2167-2181.